

Aging Behaviour and Mechanical Properties of a Solution Treated and ECAP Processed 6082 Alloy

Giuliano Angella¹, Paola Bassani², Ausonio Tuisi² and Maurizio Vedani³

¹National Research Council-Institute for Energetics and Interphases CNR-IENI, Via R. Cozzi 53, 20125 Milano, Italy

²National Research Council-Institute for Energetics and Interphases CNR-IENI, Corso Promessi Sposi 29, 23900 Lecco, Italy

³Politecnico di Milano-Dipartimento di Meccanica, Via La Masa 34, 20058 Milano, Italy

A study was carried out on the aging behaviour of a solution treated 6082 aluminium alloy deformed by equal channel angular pressing up to six passes. Aging of the so obtained ultrafine alloy was studied by DSC and TEM analyses as well as by isothermal treatments at 130, 160 and 180°C. The results showed that the formation of metastable β'' and β' precipitates were markedly anticipated and that the stable β phase was partially suppressed in the alloy processed to 4 and 6 passes, presumably due to anticipated precipitation of Si-rich particles. TEM analyses revealed that a transition in strengthening-precipitate structure occurred in the severely deformed alloy leading to a predominance of globular precipitates over the rod like phases typically found in the undeformed and aged samples. Tensile tests carried out on severely deformed and aged samples allowed to quantify the maximum strength achievable by the 6082 alloy after concurrent grain refinement and peak-hardness aging at 130°C.

(Received January 19, 2004; Accepted March 30, 2004)

Keywords: 6082 alloy, ultrafine structure, aging kinetics, mechanical properties

1. Introduction

Severe plastic deformation (SPD) is currently one of the most promising methods for processing ultrafine microstructures.¹⁻⁵⁾ Ultrafine-grained materials generally offer high strength coupled with reasonably good fracture ductility and toughness, superplastic properties at moderate temperatures and at high strain rates. SPD techniques are particularly suitable for Al alloys since these cannot be refined below a micrometer-level grain size by traditional thermo-mechanical methods. This is due to the inherent nature of the Al structure, having high stacking fault energy, thus leading to easy recovery of the dislocation structure and a reduced driving force available for recrystallisation according to conventional processes. A relatively large number of papers were recently published on mechanical properties achieved in Al alloys processed by SPD, especially using the equal channel angular pressing (ECAP) technique.⁶⁻⁹⁾ Horita and co-workers⁷⁾ investigated grain refinement by ECAP in a large number of commercial Al alloys and showed that the yield strength significantly increased after the first pressing, followed by a more reduced and gradual rise in strength with further increase of pressing passes. Fracture elongation concurrently reduced by a relatively large extent after the first pass but virtually remained the same, or even slightly increased, with further increase of imposed strain. Lowering of the tensile ductility was accounted for by the anticipated onset of necking due to the reduced strain-hardening ability of the severely deformed alloys rather than by its intrinsic loss of ductility.⁹⁾

Different approaches were adopted in published investigations when processing heat-treatable Al alloys. In a number of works, the materials were annealed, solution treated or even solution treated and aged prior to SPD.^{6,7)} However, recent works^{8,9)} demonstrated that the heavily deformed microstructure inherited from SPD processing induces accelerated aging due to enhanced diffusivity of

alloying elements at dislocations as well as new heterogeneous nucleation sites for strengthening phases at dislocation networks. Optimisation of strength and ductility can therefore be achieved by SPD processing of solution treated alloys and tailored post-SPD aging.

The issue of precipitate evolution in SPD processed microstructures was studied in detail by several authors.⁹⁻¹¹⁾ Murayama *et al.*¹⁰⁾ investigated an Al-Cu binary alloy. By careful DSC and TEM analyses they stated that the formation of GP zones and of transition θ'' precipitates is suppressed and that the precipitation of θ' and θ phases is enhanced in heavily deformed structures. These latter phases preferentially nucleated at dislocations and at grain boundaries, respectively. In the investigations carried out by Kim and co-authors^{8,9)} emphasis was also made on the accelerated kinetics of the aging process. Experimental data showed that ECAP processed 2024 and 6061 alloys experienced an accelerated aging process that was additionally attributed to a change in the diffusion coefficient by increased dislocation density of the structure.

A study on aging behaviour of an ultrafine Al alloy was described in the present paper. Solution treated samples of a commercial 6082 alloy were processed by ECAP to different degree of plastic strain at room temperature. The post-ECAP aging behaviour was investigated by DSC and by isothermal treatments at three different temperatures. TEM analyses as well as mechanical characterisation of the alloy after aging at peak hardness times allowed defining several critical aspects concerned with feasibility and convenience of aging in SPD processed alloys.

2. Experimental

A commercial 6082 Al alloy supplied in the form of extruded bars of diameter 10 mm was investigated. The alloy chemical composition is given in Table 1. Samples having a length of 100 mm were cut from the bars, solution treated in a

Table 1 Chemical composition (mass%) of the 6082 alloy investigated.

Mg	Si	Mn	Fe	Cu	Cr	Ti	Al
1.193	1.019	0.650	0.267	0.005	0.010	0.015	balance

muffle furnace at 530°C for 2 hours and water quenched.

ECAP pressing was carried out using a die with channels intersecting at an angle $\Phi = 90^\circ$ and with an external curvature angle $\Psi = 20^\circ$, corresponding to a theoretical strain of 1.05 at each pass.¹²⁾ Samples were processed at room temperature by the so-called route C (rotation by 180° of the specimen at each pass) to accumulate up to six passes. The experimental details of the ECAP facility and material processing are described elsewhere.¹³⁾

Analyses on grain structure evolution after SPD and on precipitates developed during aging was carried out on ECAP processed and post-ECAP aged samples by transmission electron microscopy (TEM). Disk samples were prepared by longitudinally cutting 1 mm thick disks from the billets, manually grinding and polishing. Twin jet electrolytic thinning was then carried out at -35°C with a 30% HNO_3 solution in methanol at 18 V. It is worth specifying that also the analysis on grain structure was performed on the same set of aged samples. As discussed in section 3.3., there is strong evidence from literature results that no significant modifications of the ultrafine grain structure occur at temperatures of the order of those here adopted for the aging treatment.

Samples of the processed alloy were subjected to Differential Scanning Calorimetry (DSC) analyses to investigate the influence of SPD on the second phase precipitation kinetics. Runs were carried out on samples having a weight of about 100 mg in a purified argon atmosphere, with a scanning rate of 30°C/min. The effects associated to transformation reactions were isolated by subtracting a baseline of high purity aluminium run.

The evolution of microhardness as a function of time during isothermal aging at temperatures of 180, 160 and 130°C was investigated and allowed to define the peak-hardness aging times of the processed alloy as a function of the number of ECAP passes experienced.

A set of processed billets was then aged to peak hardness condition at 130°C. Tensile specimens with a gauge length of 30 mm and a diameter of 6 mm were machined from the aged billets and tested at room temperature at a initial engineering strain rate of $6.7 \times 10^{-4} \text{ s}^{-1}$.

3. Results and Discussion

3.1 Grain structure after ECAP

In Fig. 1(a) set of representative TEM micrographs and of the corresponding selected-area diffraction (SAD) patterns showing the grain structure evolution as a function of ECAP passes is reported. The original grain size of the solution treated alloy was of the order of 10 μm . After the first ECAP pass, a set of parallel bands of subgrains a few hundreds of nanometers in width formed. By increasing the number of passes, the sub-boundary misalignment increased as inferred by the increased spreading of the spots of the SAD patterns. Eventually, subgrain fragmentation and further increase of

the misalignment led to an ultrafine equiaxed high-angle grain structure, with an average size of 300 nm. The above results confirm the features described by other authors on development of ultrafine structures in Al alloys and other metals processed by ECAP.^{2,4,14,15)}

3.2 Differential scanning calorimetry

Figure 2 is a summary of the recorded DSC runs as a function of number of ECAP passes experienced by the solution treated 6082 alloy. The thermogram of the unprocessed solution treated alloy match the established aging sequence of this alloy.^{16–21)} In particular, the broad exothermic peak (upward peak in the plot) at 305°C, often interpreted as two partially superimposed sub-peaks, corresponds to the formation of β'' and β' metastable precipitates at about 270°C and 330°C, respectively. More specifically, it was suggested that the sub-peak at 270°C could also be related to precipitation of tiny Si-rich particles acting as precursors for the formation of β'' phase and that at 330°C, both rod shaped β' precipitates and relatively large Si-rich precipitates are present.^{16,19–21)} A dissolution endothermic trough (downward peak in the plot) of the above phases follows at about 400°C while the second marked exothermic peak at 460°C and the corresponding endothermic trough at 520°C is related to the formation and dissolution of the equilibrium β - Mg_2Si phase, respectively.

The ECAP processed alloys feature marked differences in position and shape of the peaks. The above described broad peak related to the formation of β'' and β' phases now appears as a more narrow peak centred at 275°C, irrespective of the number of ECAP passes experienced. The formation of the stable β precipitates in the severely deformed alloy revealed to be markedly anticipated (405–415°C) and of progressively reduced intensity with respect to the unprocessed solution treated alloy. It is also worth noting that a new peak appears at about 330°C in the alloy processed to four or more passes.

Interpretation of the above mentioned changes in aging behaviour can be made on the basis of strong similarities found in the DSC curves of Al-Mg-Si alloys with excess of Si published by Gupta and co-workers.¹⁶⁾ These authors noted that an increase of the excess of Si with respect to that required to form stoichiometric Mg_2Si , made the two subpeaks related to the formation of β'' and β' more resolved, induced a hump at about 340°C, and progressively suppressed the stable β peak at 460°C. In the alloy of the present work, the excess of Si estimated according to¹⁶⁾ is only 0.26% as opposed to more than 1% excess Si considered in the study of Gupta and co-workers. However, it is believed that the increased atom mobility in the disordered SPD structure, not only accelerates the aging kinetics (as demonstrated by the shift of the peaks toward lower temperatures) but also emphasizes compositional effects as those concerned with the Mg-Si balance in the alloy. For the present alloy, on the basis of the precipitation temperatures, it can be supposed that only the β'' phase forms while β' is suppressed after ECAP. These changes are accompanied by the appearance of a hump at about 330°C for the samples processes to 4 and 6 passes and by the heavy reduction of intensity of the peak corresponding to the stable β phase. The exact phase related to the hump at 330°C remains experimentally unknown. A

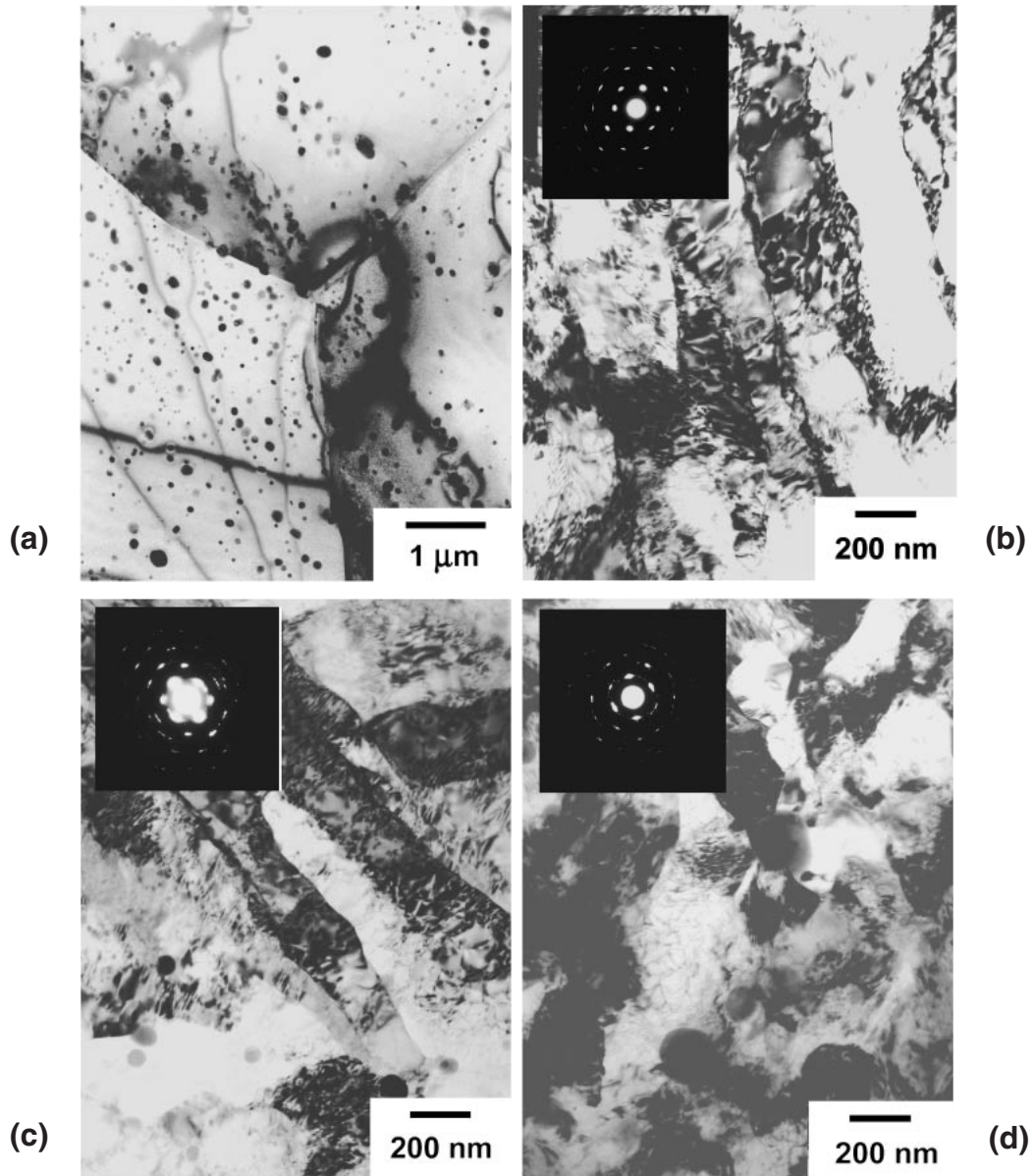


Fig. 1 Grain structure evolution of the severely deformed 6082 alloy as a function of ECAP passes: (a) solution treated sample; (b) 1 pass; (c) 2 passes; (d) 6 passes.

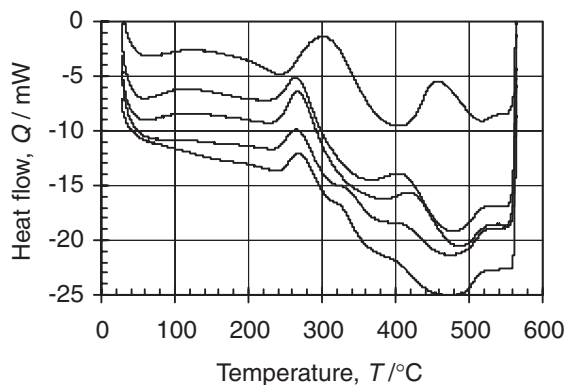


Fig. 2 DSC curves of the solution treated 6082 alloy processed to an increasing number of ECAP passes. From top to bottom curve: 0, 1, 2, 4 and 6 passes.

tentative identification of it as a Si-rich metastable phase would be supported by the detailed study published by Matsuda *et al.*²⁰⁾ who stated that β' is a competing precipitate with the so-called TYPE-B Si-rich phase featuring an ellipsoidal shape and ratio of chemical composition Si:Al:Mg = 5:4:2.

Finally, it can be supposed that the reduction of the stable β phase could be induced by the depletion of Si from the matrix caused by the anticipated formation of Si-rich precipitates, presumably at the peak located at 330°C.¹⁷⁾

3.3 Aging kinetics

Post-ECAP aging behaviour was further investigated by isothermal treatments at 130, 160 and 180°C. The evolution of microhardness as a function of aging time at the above mentioned temperatures is plotted in Fig. 3. When comparing the peak-hardness times as a function of the amount of strain experienced by the alloy prior to the aging treatment (*i.e.*

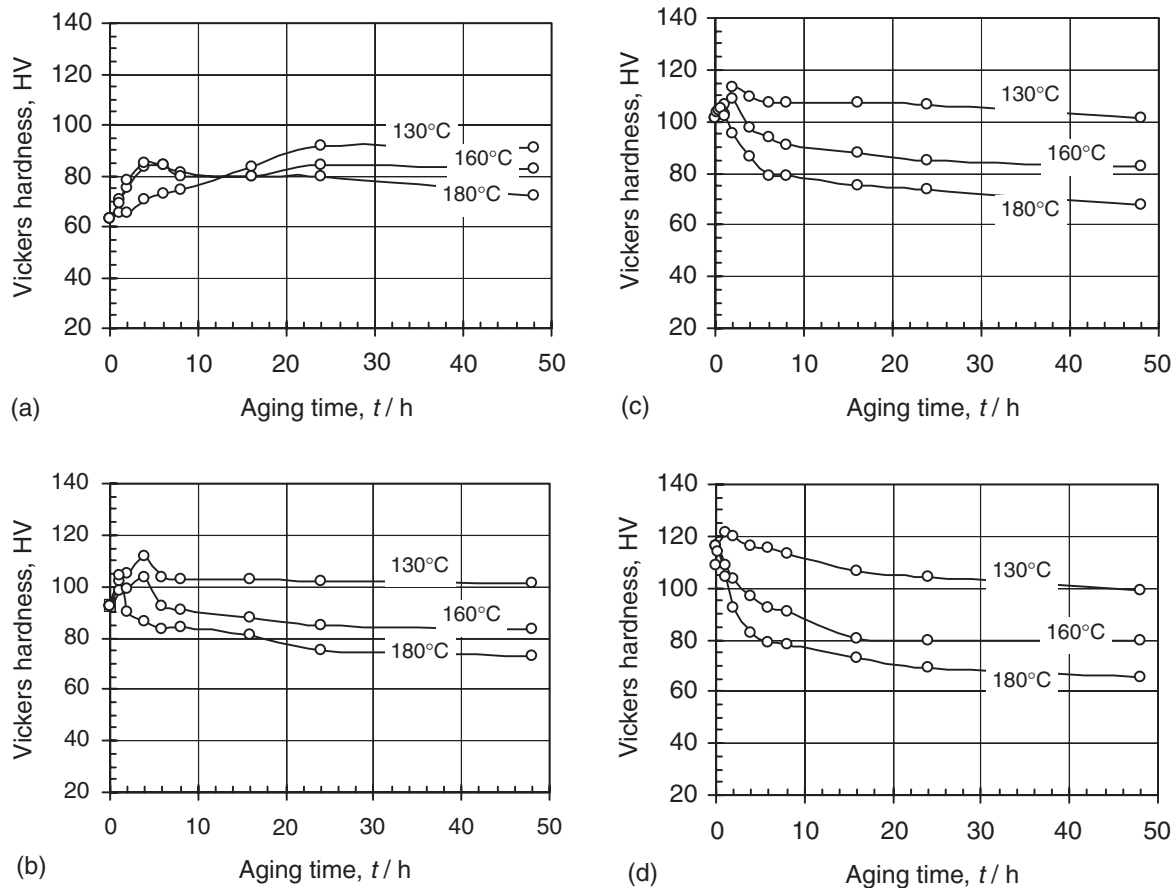


Fig. 3 Aging curves of the solution treated and ECAP processed 6082 alloy. (a) as solution treated; (b) 1 pass; (c) 2 passes; (d) 6 passes.

ECAP passes), it is readily seen that even a single ECAP pass significantly accelerates the aging kinetics, especially at the lowest aging temperature investigated. For the alloy processed to six ECAP passes, the aging kinetics at 160 and 180°C became so fast that a peak of hardness is hardly visible on the aging curves (see Fig. 3(d)).

The loss of hardness after the peaks on the curves became increasingly evident with increasing aging temperature and amount of strain experienced. It is supposed that both overaging phenomena as well as restoration of the severely deformed structure contribute to this process. Based on the microhardness values, it can be suggested that after extensive overaging (48 hours) at either 160 and 180°C, the severely deformed 6082 alloy always reached a state similar to that of the overaged unprocessed material (compare the hardness values at 48 hours for the two highest aging temperatures of the different samples).

Aging at 130°C of the SPD processed alloy revealed to be more effective by virtue of the comparatively slower kinetics and of the limited overaging effects, suggesting a reasonably high structure stability at this temperature. The hypothesis on thermal stability of the alloy structure is in good agreement with literature reports.^{22–25} Morris and co-authors²² by investigating an Al-3%Mg alloy deformed by ECAP to a total strain of about 5.6 showed that annealing of the alloy at 150°C only led to a slight reduction of dislocation density and to relaxation of cell boundaries into subgrain walls, without any other significant change in grain size or structure. Park *et*

*al.*²³) investigated grain stability of a 6061 alloy processed by accumulative roll bonding and annealed at temperatures between 100 and 500°C. Also their results demonstrated that this alloy featured a stable submicrometer-size grain-structure up to annealing at 200°C for 1 hour. An increase in the annealing temperature to 250°C led to the appearance of some large recrystallized grains.

On the basis of the above data, the aging times corresponding to peak hardness at 130°C were established and adopted to treat ECAP processed billets for more detailed microstructural analyses and for mechanical property evaluation. The selected aging times as well as the improvement in hardness of the post-ECAP aged samples over the ECAP processed (not aged) alloy are given in Table 2. It is worth noting that the precipitate strengthening generated after post-ECAP aging becomes of lower importance by increasing the amount of severe plastic deformation experienced by the sample.

Table 2 Aging times corresponding to peak hardness at 130°C of the solution treated 6082 alloy processed to an increasing number of ECAP passes and increase in hardness (Δ HV) with respect to the ECAP processed (not aged) alloy.

Number of passes	0	1	2	4	6
Aging time, t/h	24	4	2	2	1
Δ HV	29.0	20.0	11.8	5.9	4.7

3.4 Strengthening precipitates

A TEM study was carried out on the alloy strengthening precipitates found in the samples processed by ECAP to a different number of passes and post-ECAP aged at 130°C to peak-hardness condition. Figure 4 is a set of representative micrographs of several alloy conditions. The original 6082 alloy (not ECAP processed) aged to peak-hardness condition (Fig. 4(a)) featured a dispersion of 0.1 μm long rod-like phases identified as β' precipitates on the basis of their morphology^{16,17,21)} together with globular particles with an average size of 50 nm. In the ECAP processed samples (Figs. 4(b) and (c)), a recovery arrangement of dislocation was observed in the aged matrix. Moreover, the above mentioned globular particles became predominant over the rod-like precipitates. The exact composition and phase structure corresponding to the globular particles was not determined in the present investigation and it will be the subject of a future paper. However, as stated in the discussion on DSC results in section 3.2, there is evidence from literature reports^{16,21)} that

in Al-Mg-Si alloys having an excess of Si, Si-rich metastable phases form as competing precipitates with the rod-like β' phase. A similar hypothesis is therefore suggested also for the present case whereby the enhanced atom mobility in the severely deformed structure and its increased reactivity would allow the formation of a larger fraction of phases not otherwise formed in conventionally processed alloys. The above hypothesis is further supported by the good agreement found among the described transition in precipitate structure of the ECAP-processed samples, the suggested suppression of the β' peak by DSC analyses (section 3.2), and the progressive reduction of the precipitate strengthening effect measured by microhardness (section 3.3 and Table 2).

3.5 Tensile properties

Representative stress vs. strain curves of the 6082 alloy processed under different conditions and post-ECAP aged are reported in Fig. 5 while relevant tensile data are gathered in Fig. 6. From the tensile curves it is inferred that the ECAP

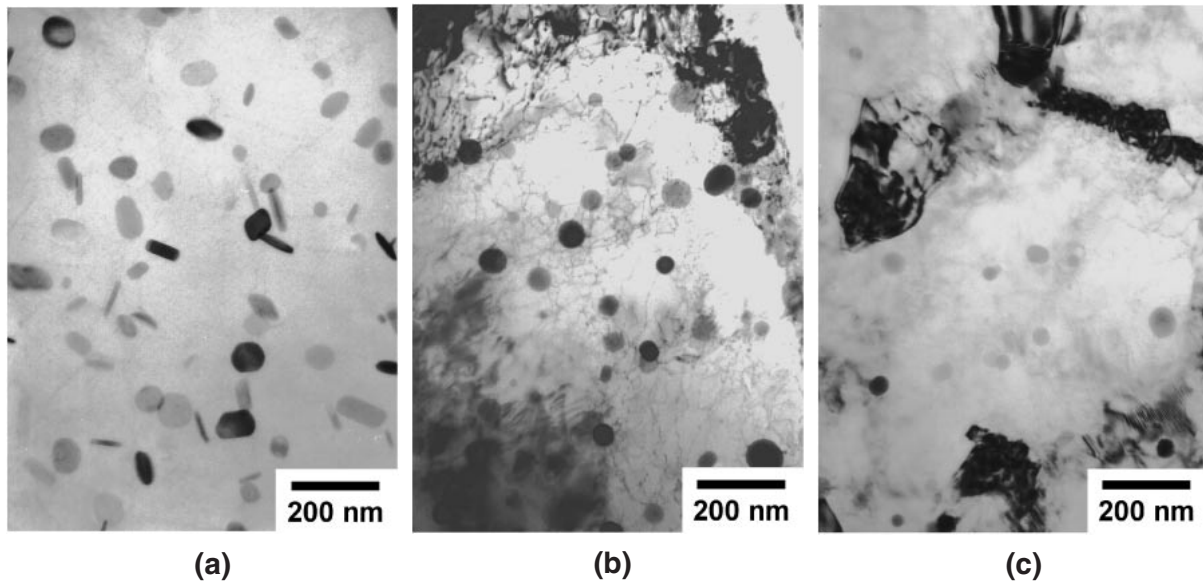


Fig. 4 Strengthening precipitate evolution of the severely deformed 6082 alloy as a function of ECAP passes: (a) unprocessed peak-aged sample; (b) 1 pass; (c) 6 passes.

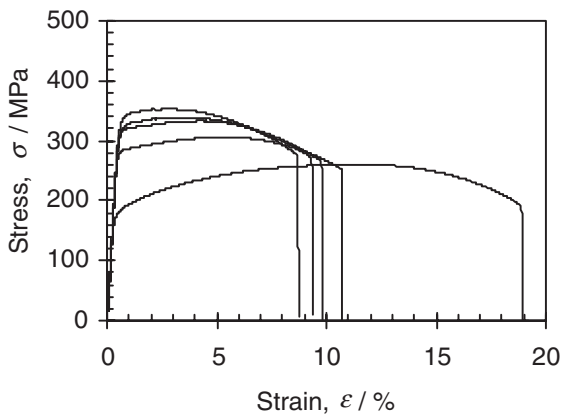


Fig. 5 Tensile curves of the solution treated ECAP processed and aged 6082 alloy. From bottom to top curve: as solution treated, 1 pass, 2 passes, 4 passes, 6 passes.

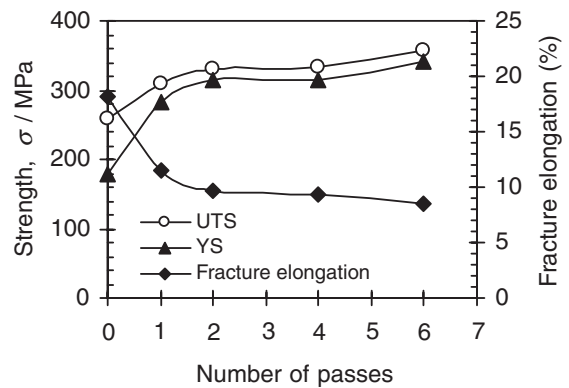


Fig. 6 Tensile properties of the solution treated ECAP processed and aged 6082 alloy as a function of passes.

processed materials underwent a dramatic increase in strength with the first pressing (the yield strength increased from 178 to 284 MPa). It is also shown that after the second pass, a tendency toward saturation of properties readily occurs. As expected, fracture elongation initially dropped from 18.1 to 11.4% but kept a satisfactory level ranging from 8 to 9% up to the sixth ECAP pass.

4. Conclusions

The aging behaviour of a 6082 alloy severely deformed by ECAP was investigated by TEM, DSC and mechanical testing. Solution treated billets were subjected to SPD at different degrees of straining and post-ECAP aged at temperatures in the range 130-180°C.

The ECAP processed alloys featured marked differences in DSC peak positions and shapes with respect to the unprocessed alloy. The peak for metastable β'' and β' precipitates was markedly anticipated and the formation of stable β phase was partially suppressed in the alloys processed to 4 and 6 ECAP passes, presumably due to anticipated precipitation of Si-rich particles.

Microhardness evolution as a function of aging time allowed to study the effect of ECAP passes on the kinetics of isothermal aging. It was stated that even a single ECAP pass significantly accelerates the aging kinetics. Aging revealed to be more effective at 130°C rather than at 160 and 180°C by virtue of the comparatively slower kinetics and of the limited overaging effects. The improvement in hardness achieved after optimised post-ECAP aging was significant for the samples subjected to a limited amount of plastic strain but became negligible after a relatively large number of ECAP passes.

TEM analyses on strengthening precipitate structure found in the ECAP processed and aged samples to peak-hardness condition revealed that globular precipitates became predominant over the rod-like transition phases in the severely deformed alloy.

Tensile tests carried out on samples processed to different numbers of ECAP passes and aged to peak-hardness showed that the alloy strength underwent a steep increase on the first ECAP pass and a near-saturation of properties on further straining. Fracture elongation significantly reduced after the first pressing. However the loss in ductility was reasonably acceptable since the typical fracture elongation values ranged from 8 to 9%.

Acknowledgements

The authors would like to thank Mr. M. Riccardi and Mr. P. Pellin for their valuable contributions in the experimental investigation.

REFERENCES

- 1) R. Z. Valiev, R. K. Islamgaliev and I. V. Alexandrov: *Prog. Mater. Sci.* **45** (2000) 103–189.
- 2) Y. Iwahashi, Z. Horita, M. Nemoto and T. G. Langdon: *Acta Mater.* **45** (1997) 4733–4741.
- 3) A. Gholinia, P. B. Prangnell and M. V. Markushev: *Acta Mater.* **48** (2000) 1115–1130.
- 4) Y. Iwahashi, M. Furukawa, Z. Horita, M. Nemoto and T. G. Langdon: *Metall. Mater. Trans.* **29A** (1998) 2245–2252.
- 5) F. H. Frohes, O. N. Senkov and E. G. Baburaj: *Mater. Sci. Engng.* **A301** (2001) 44–53.
- 6) C. S. Chung, J. K. Kim, H. K. Kim and W. Kim: *J. Mater. Sci. Engng.* **A337** (2002) 39–44.
- 7) Z. Horita, T. Fujinami, M. Nemoto and T. G. Langdon: *J. Mater. Proc. Techn.* **117** (2001) 288–292.
- 8) J. K. Kim, H. G. Jeong, S. I. Hong, Y. S. Kim and W. J. Kim: *Scr. Mater.* **45** (2001) 901–907.
- 9) W. J. Kim, C. S. Chung, D. S. Ma, S. I. Hong and H. K. Kim: *Scr. Mater.* **49** (2003) 333–338.
- 10) M. Murayama, Z. Horita and K. Hono: *Acta Mater.* **49** (2001) 21–29.
- 11) V. V. Stoyarov and R. Z. Valiev: *Proc. Int. Conf. Ultrafine Grained Materials*, ed. by R. S. Mishra, S. L. Semiatin, C. Suryanarayana, N. N. Thadhani, T. C. Lowe, Nashville, (TMS, 2000) pp. 351–360.
- 12) Y. Iwahashi, J. Wang, M. Horita, M. Nemoto and T. G. Langdon: *Scr. Mater.* **35** (1996) 143–146.
- 13) M. Vedani, P. Bassani, M. Cabibbo and E. Evangelista: *Metall. Sci. Techn.* **21** (2003) 3–9.
- 14) Z. Horita, M. Furukawa, M. Nemoto and T. G. Langdon: *Mater. Sci. Techn.* **16** (2000) 1239–1245.
- 15) Y. Iwahashi, Z. Horita, M. Nemoto and T. G. Langdon: *Acta Mater.* **46** (1998) 3317–3331.
- 16) K. Gupta, D. J. Lloyd and S. A. Court: *Mater. Sci. Engng.* **A316** (2001) 11–17.
- 17) W. F. Miao and D. E. Laughlin: *Scr. Mater.* **40** (1999) 873–878.
- 18) G. Biroli, G. Caglioti, L. Marti and G. Riontino: *Scr. Mater.* **39** (1998) 197–203.
- 19) S. B. Kang, L. Zhen, H. W. Kim and S. T. Lee: *Mater. Sci. Forum* **217–222** (1996) 827–832.
- 20) K. Matsuda, Y. Sakaguchi, Y. Miyata, Y. Uetani, T. Sato, A. Kamio and S. Ikeno: *J. of Mater. Sci.* **35** (2000) 179–189.
- 21) G. A. Edwards, K. Stiller, G. L. Dunlop and M. J. Couper: *Acta Mater.* **46** (1998) 3893–3904.
- 22) D. G. Morris and M. A. Munoz-Morris: *Acta Mater.* **50** (2002) 4047–4060.
- 23) K.-T. Park, H.-J. Kwon, W.-J. Kim and Y.-S. Kim: *Mater. Sci. Engng.* **A316** (2001) 145–152.
- 24) J. Wang, Y. Iwahashi, Z. Horita, M. Furukawa, M. Nemoto, R. Z. Valiev and T. G. Langdon: *Acta Mater.* **44** (1996) 2973–2982.
- 25) R. A. Andrievski: *J. Mater. Sci.* **38** (2003) 1367–1375.